Environmental Science and Pollution Research (2022) 29:60674–60686
https://doi.org/10.1007/s11356-022-20163-8

RESEARCH ARTICLE

Synthesis of Fe_3O_4@Phoslock® composites and the application in adsorption of phosphate from aqueous solution

You Mu[1,2] · Wuhui Luo[1,2,3,4] · Zanpeng Cui[1,2] · Meng Zhang[4] · Philip Antwi[1,2] · Dachao Zhang[1,2,3] · Sili Ren[1,2]

Received: 12 November 2021 / Accepted: 5 April 2022 / Published online: 15 April 2022
© The Author(s), under exclusive licence to Springer-Verlag GmbH Germany, part of Springer Nature 2022

Abstract

Assisted with an organosilane, Fe_3O_4@Phoslock® composites with different constituents were synthesized to separate phosphate from aqueous solution. The experimental adsorption data of kinetics and isothermal studies by the composites were well fitted by pseudo-second order and Freundlich models, respectively, suggesting the chemical and heterogeneous adsorption process, i.e., ligand exchange and precipitation. After loading of Fe_3O_4, Phoslock® became magnetic at the expense of the certain decrease of phosphate uptake from 10.4 to 8.1 mg P/g when $[P]_0 = 1.0$ mmol/L and the solid/liquid ratio of 1.0 g/L were applied. However, compared with the original Fe_3O_4 nanoparticles, Fe_3O_4@Phoslock® showed more favorable phosphate uptake and stability against pH variation. The inhibitory influence of anionic ions on phosphate adsorption by three composites followed the order: HCO_3^- > humate > SiO_3^{2-} > NO_3^- ≈ Cl^- ≈ SO_4^{2-}, while the facilitating effect of cations followed the order: Ca^{2+} > Mg^{2+} > NH_4^+. The regeneration rate was higher than 50% for all composites after recycled for 5 times by NaOH, and two of the composites successfully removed 75% phosphate from the landfill leachate treated by the Anammox process with the solid/liquid ratio of 5.0 g/L. This suggests that Fe_3O_4@Phoslock® composites would be a competitive adsorbent for phosphate removal from real wastewater.

Keywords Fe_3O_4 · Phoslock® · Phosphate · Ligand exchange · Precipitation · Organosilane

Introduction

Phosphorous (P) is the key element causing the eutrophication (Conley et al. 2009). The discharge of industrial and domestic wastewater and the intensive use of agricultural fertilizers cause the excessive P in water bodies, resulting in the rapid growth of aquatic phytoplankton and deprivation of dissolved oxygen (Cordell et al. 2009; Van Vuuren et al. 2010; Li et al. 2020). Removing P from aqueous solution is of significance and still challenging. The commonly used methods that decrease P content in water include chemical precipitation, biological accumulation, membrane separation, ion exchange, crystallization, and adsorption (Morse et al. 1998; Donnert and Salecker 1999; Rittmann et al. 2011). For the case of low P concentrations, chemical precipitation, crystallization, and biological treatment are not efficient (Aguilar et al. 2002; Sengupta et al. 2015; Bunce et al. 2018), while adsorption is suitable and shows high removal rate, simple operation, and other advantages (De Gisi et al. 2016). However, the adsorbents are generally micro- or nano-sized in order to get high surface area and favorable adsorption performance (Wendling et al. 2013; Chen et al. 2020a, b), which increases the difficulty of adsorbent separation and may cause the secondary pollution of nano-particles (Pjurova et al. 2013; Behets et al. 2020). The traditional separation methods including centrifugation and filtration require high energy consumption and cost (Tu et al. 2015). By contrast, rendering the magnetism for quick separation of the nano-sized adsorbents from

Responsible Editor: Angeles Blanco

✉ Wuhui Luo
luo070221@126.com

1 Jiangxi Key Laboratory of Mining & Metallurgy Environmental Pollution Control, Jiangxi University of Science and Technology, Ganzhou 341000, People's Republic of China

2 School of Resources of Environmental Engineering, Jiangxi University of Science and Technology, Ganzhou 341000, People's Republic of China

3 Ganzhou Technology Innovation Center for Mine Ecology Remediation, Ganzhou 341000, People's Republic of China

4 Jiangxi Academy of Environmental Sciences, Nanchang 330039, People's Republic of China

the pollutants-bearing solution assisted with the external magnetic field is feasible and widely investigated (Lai et al. 2016).

To date, Fe_3O_4 is the most applied magnetic nanoparticles due to the facile synthetic method. However, Fe_3O_4 is not stable since Fe^{2+} in the structure can be oxidized. In addition, the adsorption of P on the original Fe_3O_4 is not satisfying. Under the optimal adsorption conditions, the amount of adsorbed P on 0.05 g Fe_3O_4 in 20 mg/L P solution of 10 mL was only 3.65 mg/g (Tu et al. 2015). Therefore, Fe_3O_4 is usually covered with a layer of silicon oxide to increase its chemical stability, and the coated Fe_3O_4 nanoparticles is then grafted with P-selective materials to improve the adsorption performance, such as Fe_3O_4@SiO_2 core/shell magnetic nanoparticles functionalized with hydrous lanthanum oxide (Lai et al. 2016) and mesoporous Fe_3O_4@$mSiO_2$@mLDH composites (Li et al. 2019). However, in some cases, the coating seems not required and Fe_3O_4 was simply mixed with adsorbents to get the composite (Liu et al. 2020). The physical mixing of two solid phases, i.e., Fe_3O_4 and P adsorbents, may lead to the release of the nano-sized phases and the decrease of the recovery rate. Connecting Fe_3O_4 and another OH-bearing adsorbent by organosilane to circumvent the potential release of Fe_3O_4 is straightforward.

In various phosphorus adsorption materials (Othman et al. 2018), lanthanum modified minerals have attracted wide attention because of their high removal efficiency and selectivity. The amount of adsorbed phosphorus on La-modified diatomite was up to 37 mg/g at pH = 5 with the specific surface area increased about 82 times (Xie et al. 2013). Compared with the original vesuvianite, La doping increased the phosphorus uptake from 0.3 to 1.32 mg P/g with the initial phosphorus concentration of 1 mg/L (Li et al. 2009). The superior adsorption capacity of 147.6 mg P/g on the La-modified rectorite was obtained (Chen et al. 2020a, b). These different adsorption characteristics suggest that the phosphorus adsorption relies on the type and property of the used clay minerals (Kuroki et al. 2014). In the 1990s, the Commonwealth Scientific and Industrial Research Organization in Australia developed a lanthanum (La^{3+})-modified bentonite (Phoslock®) which was widely used to remove phosphate from various aquatic systems, such as dairy products (Kurzbaum and Shalom 2016), municipal sewage (Robb et al. 2003), reservoirs (Yamada-Ferraz et al. 2015), and lakes (Spears et al. 2013; Kuroki et al. 2014). Compared with other representative adsorbents, Phoslock® is easy to synthesize and the formed $LaPO_4$ is chemically stable and insoluble after the adsorption of orthophosphate. Thus, Phoslock® was extensively applied to tackle with the emergency pollution of P and the release of captured P in the sediment was carefully studied (Ding et al. 2018). However, considering that $LaPO_4$ may pose detrimental effects on aquatic system and La is a relatively expensive rare earth element, recovery of P-adsorbed Phoslock® from aqueous solution or sediment is of significance.

This work aims to develop the recyclable adsorbent for phosphate removal by grafting Fe_3O_4 onto Phoslock® with an organosilane as the coupling agent. The developed composites (Fe_3O_4@Phoslock®) were characterized to collect the composition and structure information, and the performance of the Fe_3O_4@Phoslock® for phosphate removal was fully investigated, including kinetics, isotherms, influences of pH and coexisting ions, and regeneration.

Materials and methods

Chemicals and reagents

Phoslock® was provided by Phoslock Water Solutions Ltd (Changxing, Zhejiang, China), and the element composition was determined by X-ray fluorescence (O 28.96%, Si 25.85%, Al 6.43%, Ca 1.53%, La 1.36%, K 1.35%, Cl 1.30%, Fe 1.29%, Mg 1.20%, Na 0.50%, P 0.02%, others 0.41%, and the ignition loss 29.80%). Fe_3O_4 and organosilane were synthesized in laboratory. All phosphate-bearing solutions were prepared using ultrapure water, and the reagents are of analytically pure and directly used without further treatment.

Synthesis of Fe_3O_4@Phoslock®

Fe_3O_4 was synthesized by co-precipitation with Fe^{3+} and Fe^{2+} at the molar ratio of 2.0 under the alkaline condition (Yoon et al. 2014). To be specific, 4.410 g of $FeCl_3{\cdot}6H_2O$ and 1.614 g of $FeCl_2{\cdot}4H_2O$ were dissolved in 200 mL ultrapure water and the solution pH was adjusted to 10 ~ 11 using 2 mol/L NaOH. After aging at 85 °C in the oil bath for 1 h, the synthesized Fe_3O_4 was cooled to room temperature, washed with ultrapure water until neutral, separated from the water by magnet, freeze-dried, and ground for further use.

To preparation the organosilicon quaternary ammonium salt (organosilane) (Mebes and Ludi 1989), 1.0 g of 3-chloropropylmethyldimethoxysilane, 1.1 g of N,N-dimethyldodecyl amine, and 0.1 g of sodium iodide were successively added into a flask containing 100 mL of ethanol. The solution was then heated to boiling at 90 °C, refluxed and stirred for 2 days, and cooled to room temperature. After filtration, the solvent was removed by vacuum distillation to obtain a yellowish viscous liquid.

3.0 g of Phoslock® was dispersed in 100 mL of anhydrous ethanol for 30 min, and then 3.0 g of organosilane was slowly added into the suspension and mixed vigorously at 85 °C for 6 h. To further load the magnetism to organosilane-fabricated Phoslock®, 3.0 g of Fe_3O_4 was added and the mixture was maintained at 85 °C for extra 14 h. The final composite was thoroughly washed by ethanol and

ultrapure water, freeze-dried, and labeled as $M_3O_3P_3$. With the similar protocol, another two composites with different mass ratios of Fe_3O_4, organosilane, and Phoslock® were prepared, namely, $M_3O_3P_{1.5}$ and $M_2O_4P_4$.

Characterization

The carbon contents of samples were determined on a CS744 elemental analyzer (LECO, Michigan, USA). The iron and lanthanum concentrations of composites were determined by an inductively coupled plasma mass spectrometer (Agilent 8800, Agilent Technologies, USA) and a single channel scan inductively coupled plasma emission spectrometer (ULTIMA 2, HORIBA, Japan), respectively. X-ray diffraction (XRD) was carried out on an Empyrrean X-ray diffractometer (PANalytical, Almelo, Netherlands) equipped with a Cu Kα radiation source ($\lambda = 1.5418$ Å at 40 kV and 40 mA). Field emission scanning electron microscopy (FESEM, Sigma 300, Zeiss, Germany) equipped with an energy dispersive X-ray spectrometer (EDX) was applied to characterize the surface morphology and elemental distribution of sample at an accelerating voltage of 5 kV. The magnetic property was measured using a vibrating sample magnetometer (VSM, LakeShore 7404, USA) at room temperature with a field measurement range of ± 2.0 kOe.

Batch adsorption experiments

Adsorption kinetics

A batch of vials containing 20 mg of adsorbent and 20 mL of 0.1 or 1.0 mmol/L phosphate-bearing solution were shaken at room temperature (200 rpm). At different times ($t = 10$, 20, 30, 45, 60, 90, 120, and 180 min), two parallel vials were fetched out and the mixture were filtered to measure the residual concentration of phosphate in the solution using the spectrophotometric method (Liu et al. 2018) (L5, INESA, Shanghai, China). The amount of P adsorbed (Q_t, mg /g) was calculated by Eq. (1).

$$Q_t = \frac{\left(C_0 - C_t\right) \times V}{m} \tag{1}$$

where V is the volume of solution (L), m represents the mass of adsorbents (g), and C_0 and C_t are the concentrations of P in solution at the beginning and at time t (mg/L), respectively.

The experimental results were fitted with pseudo first- and second-order models (Eqs. (2) and (3)) (Nodeh et al. 2017):

Pseudo-first-order model

$$Q_t = Q_e - \frac{Q_e}{exp\left(k_1 t\right)} \tag{2}$$

Pseudo-second-order model

$$Q_t = \frac{Q_e^2 k_2 t}{1 + k_2 Q_e} \tag{3}$$

where Q_e and Q_t are the P uptake at equilibrium and at time t (mg/g), respectively, and k_1 (1/min) and k_2 (g/(mg·min)) are the rate constants.

Adsorption isotherms

To achieve the maximum uptake of phosphate on the synthesized adsorbents, a series of solutions with different phosphate concentrations ranged from 0.05 to 5.0 mmol/L were prepared. Per the similar protocol of kinetics study, the phosphate concentrations in the solutions after shaking for 24 h were determined and applied to calculate the phosphate uptake. The Langmuir and the Freundlich models (Długosz et al. 2018) were applied to fit the adsorption results.

Langmuir model

$$Q_e = \frac{Q_{max} k_L C_e}{1 + k_L C_e} \tag{4}$$

Freundlich model

$$Q_e = k_F C_e^{\ 1/n} \tag{5}$$

where Q_e is the P concentration at equilibrium (mg/g), k_L denotes the Langmuir constant related to the affinity of binding sites (L/mg), Q_{max} refers to the adsorption capacity (mg/g), k_F represents the Freundlich constant related to adsorption capacity ((mg/g)/(mg/L)$^{1/n}$), and $1/n$ is the constant related to the adsorption density.

Influence of pH and coexisting ions

To investigate the influence of pH on the adsorption of phosphate, the solutions of 0.1 mmol/L phosphate at different pH (2 ~ 11) were prepared, and with the solid/liquid ratio of 20 mg/20 mL, the residual phosphate concentrations were determined after shaking for 180 min. Similarly, to study the influence of coexisting ions, the solutions containing 0.1 mmol/L phosphate and 1.0 mmol/L anions (including NO_3^-, Cl^-, SO_4^{2-}, HCO_3^-, SiO_3^{2-}, and humate) or cations (including Ca^{2+}, Mg^{2+}, and NH_4^+) were prepared, and the P uptakes in these systems were measured and calculated.

Regeneration and reuse

The P-saturated composites were regenerated by 1.0 mol/L NaOH with the solid/liquid ratio of 50 mg/mL (Hokkanen et al. 2018). After desorption, the solid was washed with ultrapure water to neutral, filtered, freeze-dried, and ground. Sequentially, the regenerated composite was applied to conduct the next adsorption experiment. Such an experiment was repeated for five cycles, the regeneration efficiency (η, %) was calculated by Eq. (6).

$$\eta_n = \frac{Q_n}{Q_0} \times 100\% \tag{6}$$

where Q_0 and Q_n are P uptakes at the beginning and after regenerated for the n times (mg/g), respectively.

Application test

The synthesized composites were used to remove phosphate in the landfill leachate treated by Anammox. The initial P concentration and pH of the solution were approximately 3.5 mg/L and 9.1, respectively. With the similar adsorption conditions abovementioned, the influence of dosage on phosphate removal from the treated landfill leachate was explored using the solid/liquid ratios of 20, 30, 40, and 50 mg/10 mL. The removal rate of P (R, %) was calculated by Eq. (7).

$$R = \frac{C_0 - C_e}{C_0} \times 100\% \tag{7}$$

where C_0 and C_e (mg/g) are the initial and equilibrium concentrations of P in solution, respectively.

Results and discussion

Physicochemical characteristics

The content of Fe, C, and La in Phoslock® and Fe_3O_4@Phoslock® composites are shown in Table 1. The content of Fe_3O_4, organosilane, and La in the composites can be calculated by Eqs. (8), (9), and (10), respectively.

$$n_M = \frac{w_{Fe} - 0.23w}{N_{Fe}M_{Fe}} \tag{8}$$

where n_M is the content of Fe_3O_4 (mol/g); w_{Fe} refers to the Fe content in percentage (%); w denotes the approximate mass ratio of Phoslock® in composites, i.e., 1.5/7.5 for $M_3O_3P_{1.5}$, 3/9 for $M_3O_3P_3$, and 4/10 for $M_2O_4P_4$; 0.23 represents the percentage of Fe content in Phoslock® (%); N_{Fe} is the number of Fe_3O_4 molecular Fe ($N_{Fe}=3$); and M_{Fe} is the relative atomic mass of an iron atom (56 g/mol).

$$n_O = \frac{w_C - 0.62w}{N_C M_C} \tag{9}$$

where n_O represents the content of organosilane (mol/g), w is same as Eq. (8), 0.62 represents the impurity C content in Phoslock® in percentage (%), N is the number of C in a organosilane molecule ($N_C=20$), and M_C is the relative atomic mass of carbon atom (12 g/mol).

$$n_P = \frac{w_{La}}{M_{La}} \tag{10}$$

where n_P is the content of La in the modified adsorbent (mol/g), w_{La} is the La content of the composite in percentage (%), and M_{La} is the atomic mass of La (139 g/mol).

Based on the final molar contents of Fe_3O_4, organosilane, and La, three composites are renamed for comparison (Table 1). Compared with Phoslock®, the content of Fe and C elements increased significantly after modification, indicating that both organosilane and Fe_3O_4 were successfully loaded onto Phoslock®. Notably, the contents of organosilane in the composites were proportionally increased with the dosage of Phoslock®, which can be ascribed to the ion exchange with La^{3+} ions and condensation reactions with the hydroxyl groups in Phoslock®. In principle, the content of Fe_3O_4 in final composite should be increased with the dosage of organosilane due to the condensation reactions, while the opposite results were observed. This suggests that the loading of organosilane was governed by Phoslock® rather than Fe_3O_4. Organosilane molecules intercalated into the interlayer space of Phoslock® and anchored on the internal surface via electrostatic interactions, leaving only a small amount of organosilane in solution for the condensation with

Table 1 Composition of Fe_3O_4@Phoslock® composites

Name	w_{Fe} (%)	w_C (%)	w_{La} (%)	Fe_3O_4 (mmol/g)	Organosilane (mmol/g)	La (mmol/g)	Rename
Phoslock®	0.23	0.62	4.23	-	-	-	-
$M_3O_3P_{1.5}$	44.62	4.32	1.39	2.65	0.175	0.100	$M_{26.5}O_{1.7}P_1$
$M_3O_3P_3$	36.05	5.37	2.00	2.14	0.215	0.144	$M_{14.9}O_{1.5}P_1$
$M_2O_4P_4$	21.38	7.01	2.75	1.27	0.282	0.198	$M_{6.4}O_{1.4}P_1$

Fe_3O_4. Notably, due to the steric hindrance, the micro-sized Fe_3O_4 is hardly to intercalate into the nano-sized interlayer space to condense with the anchored organosilane. In other words, mixing organosilane and Phoslock® at the first stage reduced the reaction possibility of organosilane with Fe_3O_4. As a result, the loading of Fe_3O_4 on the external surface or in the "house-of-card" structure through physical interactions may account for the decreasing contents.

To achieve the structural information, the XRD patterns of samples were collected and shown in Fig. 1. The fine crystal structure of the original Phoslock® was evidenced in Fig. 1(a), while the diffraction peaks at the 2θ values of 20.9°, 26.5°, and 50.1° suggest the presence of quartz (SiO_2, PDF#85–0930). Compared with the original Phoslock®, the Fe_3O_4@Phoslock® composites exhibited new diffraction peaks at 2θ values of 30.1°, 35.5°, and 62.6°, which are assigned to Fe_3O_4 (PDF#75–0033) and still maintained after phosphate adsorption. This further verifies that Fe_3O_4 was stably loaded onto Phoslock®. As reported, Fe_3O_4 can separate phosphate from water mainly through complexation or ligand exchange with hydroxyl groups on the surface without destruction of the crystal structure (Moharami and Jalali 2014). To confirm the intercalation of organosilane, the XRD patterns at low 2θ values are recorded (Fig. 1(b)). The 2θ of 001 reflection was significantly shifted from 5.8 to 3.8° after the loading of organosilane and Fe_3O_4, corresponding to the increase of d_{001} value from 1.54 to 2.30 nm (Chen et al. 2019). This should be attributed to the above-mentioned ion exchange between organosilane cations and the La^{3+} ions in the interlayer space of Phoslock® (Luo et al. 2020). After phosphate adsorption, the interlayer distance of the adsorbents was not changed, suggesting that the intercalated organosilane were stably trapped between the layers and hardly released.

Doping of Fe_3O_4 on Phoslock® grants the magnetism on the final composites. As shown in Fig. 2, the magnetic hysteresis loops confirm the excellent superparamagnetism of the synthesized composites (Wong et al. 2020). Compared with the original Fe_3O_4 nanoparticles that have a saturation magnetization of 61.7 emu/g, $M_{26.5}O_{1.7}P_1$, $M_{14.9}O_{1.5}P_1$, and $M_{6.4}O_{1.4}P_1$ show the saturation magnetization of 42.0, 33.3, and 17.3 emu/g, respectively. The decrease of the saturation magnetization is a common phenomenon in the modified magnetic materials (Peng et al. 2012; Lai et al. 2016), because Fe_3O_4 was only partially grafted as a magnetic

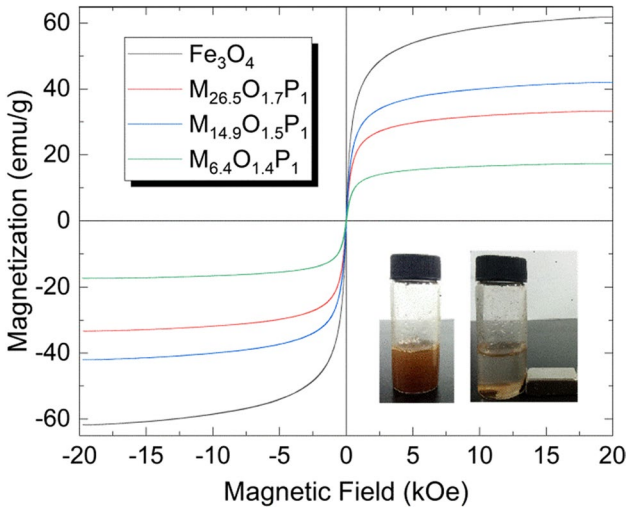

Fig. 2 Magnetic hysteresis loops of various magnetic materials

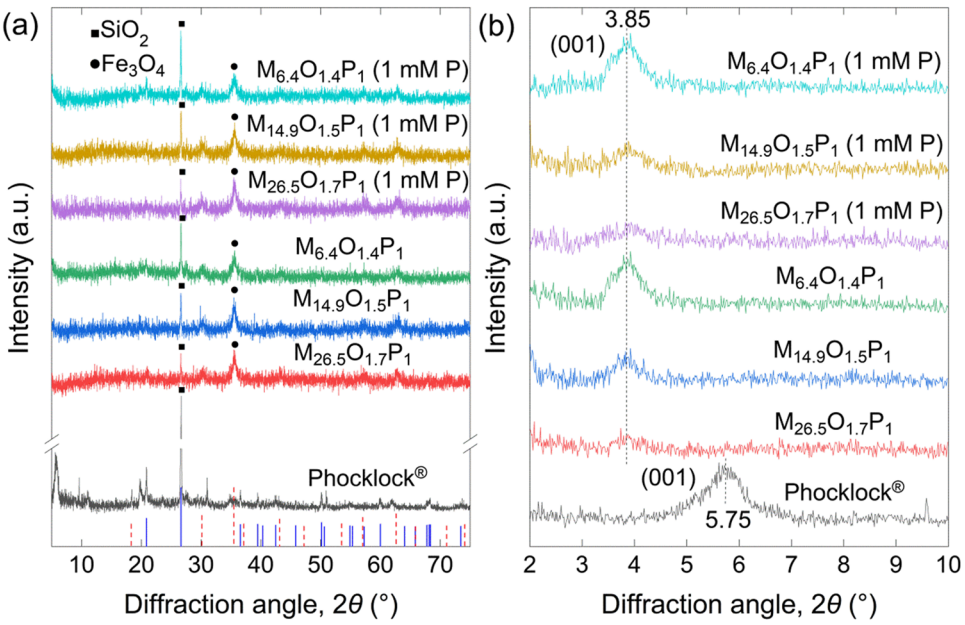

Fig. 1 XRD patterns of the samples

constituent on the non-magnetic Phoslock®. In the inset of Fig. 2, $M_{6.4}O_{1.4}P_1$ with the lowest saturation magnetization can be rapidly attracted by the applied magnetic field, which was quickly re-dispersed with a facile agitation after the dismissal of the magnetic field. This implies that Fe_3O_4@Phoslock® can be readily recovered and feasibly applied in the practical adsorption process.

Adsorption characteristics of Fe_3O_4@Phoslock® for phosphate

Adsorption kinetics

The phosphate uptake on the composites as a function of time is depicted in Fig. 3. For the initial phosphate concentrations of 0.1 and 1.0 mmol/L, it takes 60 and 90 min to achieve the equilibrium, respectively. Three composites showed the similar adsorption kinetics and phosphate uptake at the concentration of 0.1 mmol/L due to enough adsorption sites. However, at high phosphate concentration, the amount of adsorbed phosphate of $M_{6.4}O_{1.4}P_1$ was lower than that of $M_{14.9}O_{1.5}P_1$ and $M_{26.5}O_{1.7}P_1$, because the lower content of Phoslock® (La^{3+}) and the presence of organosilicon film (explained in "Adsorption mechanism") in $M_{6.4}O_{1.4}P_1$. The fitting parameters of pseudo-first order and pseudo-second order models are summarized in Table 2. The correlation coefficients (R^2) imply the better fitting of the pseudo-second order model with respect to the pseudo-first order model, which is in good agreement with some reported phosphate adsorbents (Yang et al. 2013; Moharami and Jalali 2014). In addition, the calculated Q_e values of the pseudo-second order model were closer to the experimental data. These results suggest that the chemisorption was the rate-limiting processes (Moharami and Jalali 2014; Tu et al. 2015) and adsorption of phosphate might be attributed to the ligand exchange with hydroxyl groups and $LaPO_4$ precipitation (Haghseresht et al. 2009; Moharami and Jalali 2014).

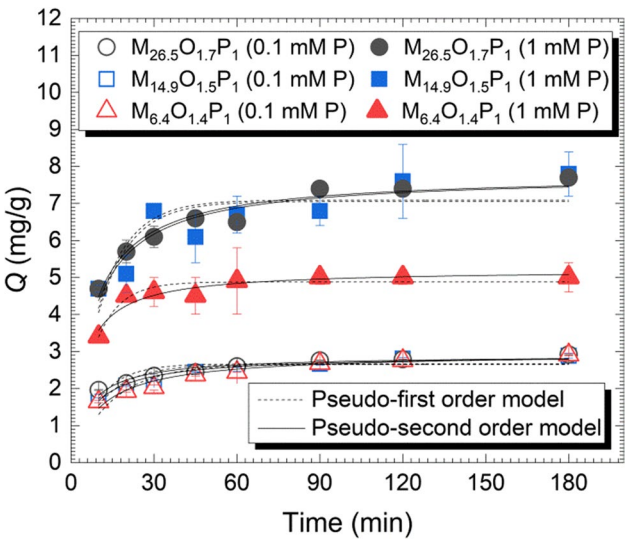

Fig. 3 Adsorption kinetics of phosphate on Fe_3O_4@Phoslock® composites (m = 20 mg, V = 20 mL, $[P]_0$ = 0.1 or 1 mmol/L, T = 25 °C, without pH control)

Adsorption isotherms

Fitting of the isothermal adsorption data using the Langmuir and Freundlich models are depicted in Fig. 4, and the corresponding parameters are summarized in Table 3. The adsorption capacities of P calculated by the Langmuir equation (Eq. (4)) are 20.6, 15.9, and 16.9 mg/g for $M_{26.5}O_{1.7}P_1$, $M_{14.9}O_{1.5}P_1$, and $M_{6.4}O_{1.4}P_1$, respectively. However, the fitting results of Q_{max} were different from the experimental data, which was ascribed to the mismatch of phosphate adsorption with the ideal adsorption conditions assumed by the Langmuir model (Ghosal and Gupta 2017). The correlation coefficients (R^2) (Table 3) of the Freundlich model are much closer to 1.0 with respect to that of the Langmuir model, suggesting the better fitting. This is caused by the heterogeneous adsorption sites on Fe_3O_4@Phoslock® composites, which is consistent with the fitting results of pollutants adsorption on some reported multi-phase composites (Hu et al. 2017; Guerra et al. 2020). The value of 1/n in the Freundlich model was ranged from 0.1 to 1, indicating that the adsorption process is easy to occur (Wen et al. 2013; Li et al. 2019).

Table 2 Parameters of the kinetic models used for the fitting of different concentrations of phosphate onto Fe_3O_4@Phoslock®

Adsorbent	C_0	Pseudo-first-order			Pseudo-second-order		
	(mmol/L)	Q_e (mg/g)	k_1 (1/min)	R^2	Q_e (mg /g)	k_2 (g/(mg·min))	R^2
$M_{26.5}O_{1.7}P_1$	0.1	2.67 ± 0.09	0.104 ± 0.020	0.658	2.90 ± 0.07	0.058 ± 0.011	0.915
$M_{14.9}O_{1.5}P_1$		2.65 ± 0.09	0.088 ± 0.016	0.747	2.91 ± 0.06	0.047 ± 0.007	0.948
$M_{6.4}O_{1.4}P_1$		2.65 ± 0.12	0.068 ± 0.013	0.761	2.95 ± 0.09	0.033 ± 0.006	0.934
$M_{26.5}O_{1.7}P_1$	1.0	7.05 ± 0.30	0.086 ± 0.019	0.690	7.76 ± 0.34	0.017 ± 0.005	0.835
$M_{14.9}O_{1.5}P_1$		7.09 ± 0.23	0.089 ± 0.015	0.780	7.78 ± 0.17	0.018 ± 0.003	0.949
$M_{6.4}O_{1.4}P_1$		4.88 ± 0.08	0.119 ± 0.012	0.903	5.21 ± 0.10	0.042 ± 0.007	0.917

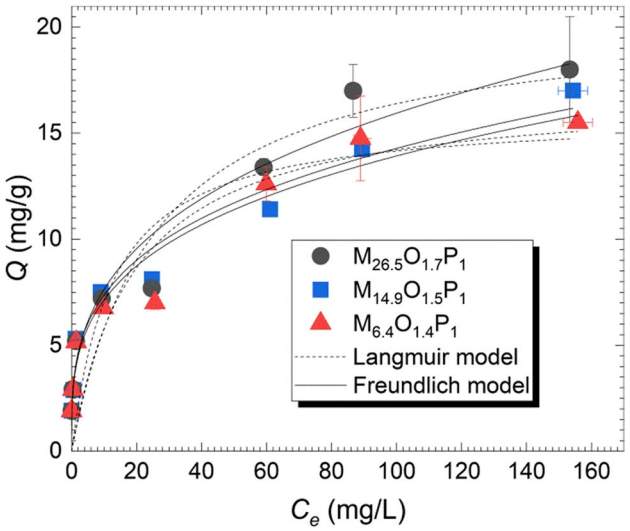

Fig. 4 Adsorption isotherms of phosphate on Fe_3O_4@Phoslock® composites (m = 20 mg, V = 20 mL, T = 25 °C, t = 24 h, without pH control)

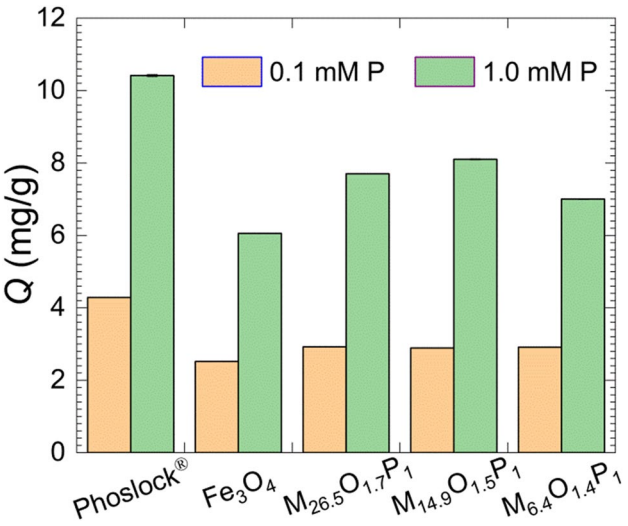

Fig. 5 Comparison of phosphate adsorption on Phoslock®, Fe_3O_4, and Fe_3O_4@Phoslock® composites (m = 20 mg, V = 20 mL, $[P]_0$ = 0.1 or 1.0 mmol/L, T = 25 °C, t = 3 h, without pH control)

Comparison of Fe_3O_4@Phoslock® with precursors

As shown in Fig. 5, phosphate removal from aqueous solutions was compared among Fe_3O_4, Phoslock®, and Fe_3O_4@Phoslock® composites. The relatively low phosphate uptake of Fe_3O_4 synthesized in the lab was consistent with the previously reported results (Daou et al. 2007; Yoon et al. 2014; Moharami and Jalali 2014; Tu et al. 2015), while Phoslock® showed relatively high phosphate uptake and was close to the reported results (Haghseresht et al. 2009). Under the same experimental conditions, the amount of adsorbed phosphate was in an order of Phoslock® > $M_{14.9}O_{1.5}P_1$ > $M_{26.5}O_{1.7}P_1$ > $M_{6.4}O_{1.4}P_1$ > Fe_3O_4, regardless of the initial concentration of phosphate (0.1 or 1.0 mmol/L). The adsorption capacity of $M_{26.5}O_{1.7}P_1$ (20.6 mg/g; Table 3) is competitive with respect to some recently reported adsorbents, such as Lanthanum (La) Modified Bentonite (8.51 mg/g) (Ding et al. 2018), and La(III)-Modified Bentonite (14.0 mg/g) (Kuroki et al. 2014). Although the phosphate uptake of the composite was decreased slightly with respect to the original Phoslock®, the composite possesses the magnetism and can be quickly recycled.

Effect of solution pH

As shown in Fig. 6, uptake of phosphate by three composites shows the similar tendency with solution equilibrium pH, where the amount of adsorbed phosphate was maintained in the acid conditions (pH of 2.0 ~ 6.8) and started to plummet until pH approximately 7.0. The influence of pH on phosphate adsorption should be attributed to the change of surface charge, competition with hydroxide ions, and variation of phosphate species (Fig. 6(b)). According to a previous study (Moharami and Jalali 2014), phosphate uptake by Fe_3O_4 was gradually decreased with the solution pH (removal percentage of ~ 65% at pH 2.0 and that of ~ 35% at pH 8.0), different from the observed trend on Fe_3O_4@Phoslock® composites (Fig. 6). This can be rationalized by the stable performance of Phoslock®, showing phosphate uptake around 4.4 mg/g in the pH 5 ~ 7 with $[P]_0$ = 1 mg/L (Ross et al. 2008). The point of zero charge of Fe oxides generally ranges from pH 7 to 9 (Wendling et al. 2013) and the formation of hydroxyl species of La^{3+} (Ross et al. 2008), which might account for the rapid drop of phosphate uptake in alkaline conditions.

Table 3 Parameters of the Langmuir model and Freundlich model for the isotherms on Fe_3O_4@Phoslock®

Adsorbent	Langmuir model			Freundlich model		
	Q_{max} (mg/g)	k_L (L/mg)	R^2	k_F ((mg/g)/(mg/L)$^{1/n}$)	n	R^2
$M_{26.5}O_{1.7}P_1$	20.6 ± 3.7	0.039 ± 0.02	0.855	3.67 ± 0.7	3.14 ± 0.4	0.954
$M_{14.9}O_{1.5}P_1$	15.9 ± 2.3	0.080 ± 0.03	0.806	3.81 ± 0.5	3.49 ± 0.4	0.966
$M_{6.4}O_{1.4}P_1$	16.9 ± 3.0	0.052 ± 0.03	0.819	3.67 ± 0.6	3.45 ± 0.5	0.949

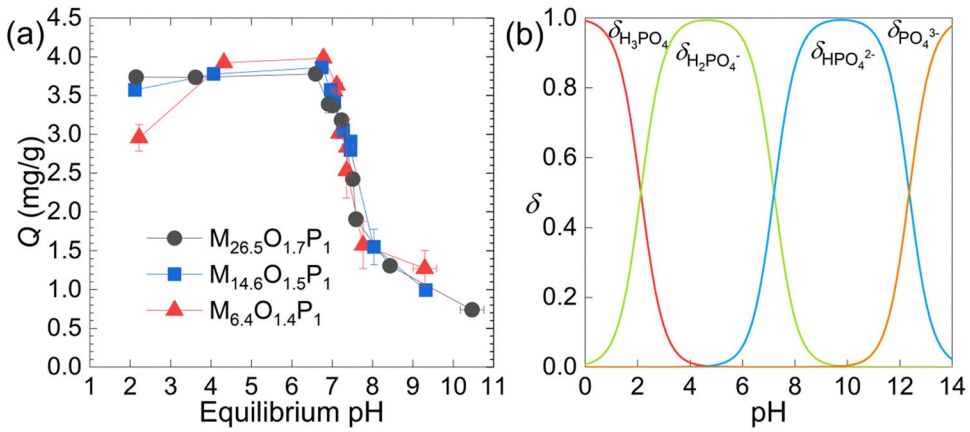

Fig. 6 (a) Effect of pH on phosphate adsorption on Fe_3O_4@Phoslock® composites (m = 20 mg, V = 20 mL, $[P]_0$ = 0.1 mmol/L, T = 25 °C, t = 3 h) and (b) speciation of phosphate as a function of pH

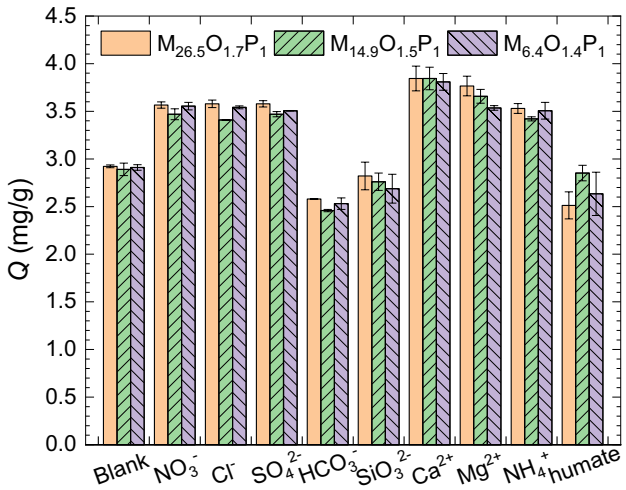

Fig. 7 Effect of co-existing ions on the adsorption of phosphorus by Fe_3O_4@Phoslock® composites (m = 20 mg, V = 20 mL, $[P]_0$ = 0.1 mmol/L, [co-existing ion] = 1 mmol/L, T = 25 °C, t = 3 h, initial pH range 5.4 ~ 7.8)

Effects of coexisting ions

The effects of naturally present substances on the adsorption of phosphate by Fe_3O_4@Phoslock® composites are shown in Fig. 7. The inhibitory influence of anionic ions on phosphate adsorption followed the order: HCO_3^- > humate > SiO_3^{2-} > NO_3^- ≈ Cl^- ≈ SO_4^{2-}, while the facilitating effect of cations followed the order: Ca^{2+} > Mg^{2+} > NH_4^+. The equilibrium pH values of the HCO_3^-, SiO_3^{2-}, and humic-bearing systems were 7.8, 7.3, and 7.4, respectively, while the pH ranged from 6.9 to 7.1 for other systems. Because phosphate uptake is pH-sensitive (Fig. 6), the small pH difference might result in the significant uptake inhibition. In addition, the former three anions might compete with phosphate to interact with hydroxyl groups and La^{3+} in Fe_3O_4@Phoslock® composites through the hydrogen-bond and inner-sphere complex interactions. In general, adding NO_3^-, Cl^-, and SO_4^{2-} increased the ionic strength and would weaken the electrostatic interactions of phosphate with $-R_4N^+$. Thus, the negligible inhibition of these ions on phosphate uptake implies that electrostatic interaction was not the main adsorption mechanism. Compared with anions, the presence of Ca^{2+}, Mg^{2+}, and NH_4^+ might enhance the electrostatic attractions between the composites and phosphate. The enhanced phosphate adsorption on goethite in the presence of Ca^{2+} was reported due to the electrostatic interactions among phosphate, Ca^{2+} and the goethite mineral surface, i.e., Ca^{2+} bridging (Wendling et al. 2013). The composites show high selectivity for phosphate in the presence of common cations and anions, implying the promising potential for application in real sewage.

Regeneration and reuse

At high pH hydroxide ions significantly inhibit phosphate adsorption (Fig. 6), suggesting that NaOH would be a favorable reagent for the composites regeneration. After regenerated by 1.0 mol/L NaOH for 5 cycles, uptake of phosphate was reduced by 28%, 48%, and 34% for $M_{26.5}O_{1.7}P_1$, $M_{14.9}O_{1.5}P_1$, and $M_{6.4}O_{1.4}P_1$, respectively (Fig. 8). Phosphate captured by Fe_3O_4 via inner-sphere complex and in $LaPO_4$ precipitate were desorbed, while during the regeneration process, some of La^{3+} were transformed into nano-sized $La(OH)_3$ in the alkaline solution and lost. Thus, the remarkable decreases of phosphate uptake in the headmost cycles were observed, while the small drops in the latter cycles suggested the favorable regeneration performance, especially for $M_{26.5}O_{1.7}P_1$. Considering the high phosphate concentration in the solution produced from the regeneration processes (6.3 ~ 21 mmol/L), precipitating phosphate through feeding Ca^{2+}, Mg^{2+}, and NH_4^+ salts in forms of hydroapatite and struvite to recovery phosphorus as fertilizer is applicable (Kuzawa et al. 2006; Desmidt et al. 2015). In addition, the solution is still strongly basic after phosphate precipitation. Therefore, it can be applied to precipitate heavy metal

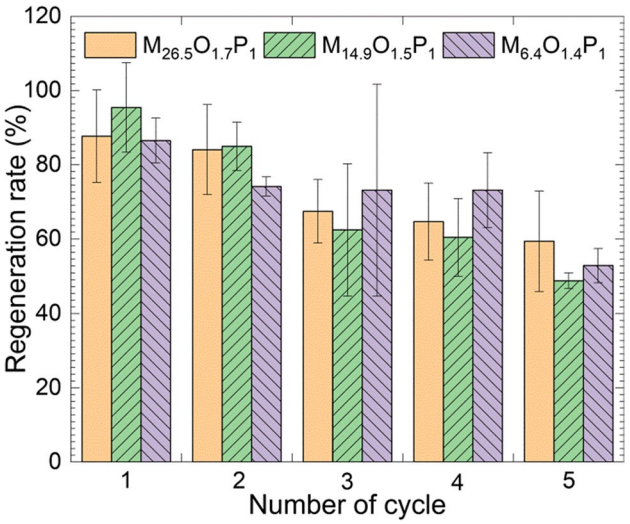

Fig. 8 Regeneration performance of Fe_3O_4@Phoslock® composites

cations in the industrial wastewater or reused as the regenerating agent after filtration.

Adsorption mechanism

The morphology and element mapping of $M_{26.5}O_{1.7}P_1$, $M_{14.9}O_{1.5}P_1$, and $M_{6.4}O_{1.4}P_1$ are presented in Fig. 9. SEM images showed the coverage of spherical or near-spherical Fe_3O_4 nanoparticles on the edge and/or surface of Phoslock®, and the similar phenomenon was also observed on the kaolin/Fe_3O_4 composites synthesized by the co-precipitation method (Liu et al. 2020). Different from $M_{26.5}O_{1.7}P_1$ and $M_{14.9}O_{1.5}P_1$, there is a thin film on the surface of $M_{6.4}O_{1.4}P_1$. The smallest content of Fe_3O_4 in $M_{6.4}O_{1.4}P_1$ (Table 1) provided the least hydroxyl groups and indirectly facilitated the silylanization of organosilane molecules. In addition, the content of Cl on the surface of $M_{6.4}O_{1.4}P_1$ is significantly higher than that of the other two analogues. Thus, a layer of organosilane film might be formed on the surface, similar as the silica-supported polyether polysiloxane quaternary

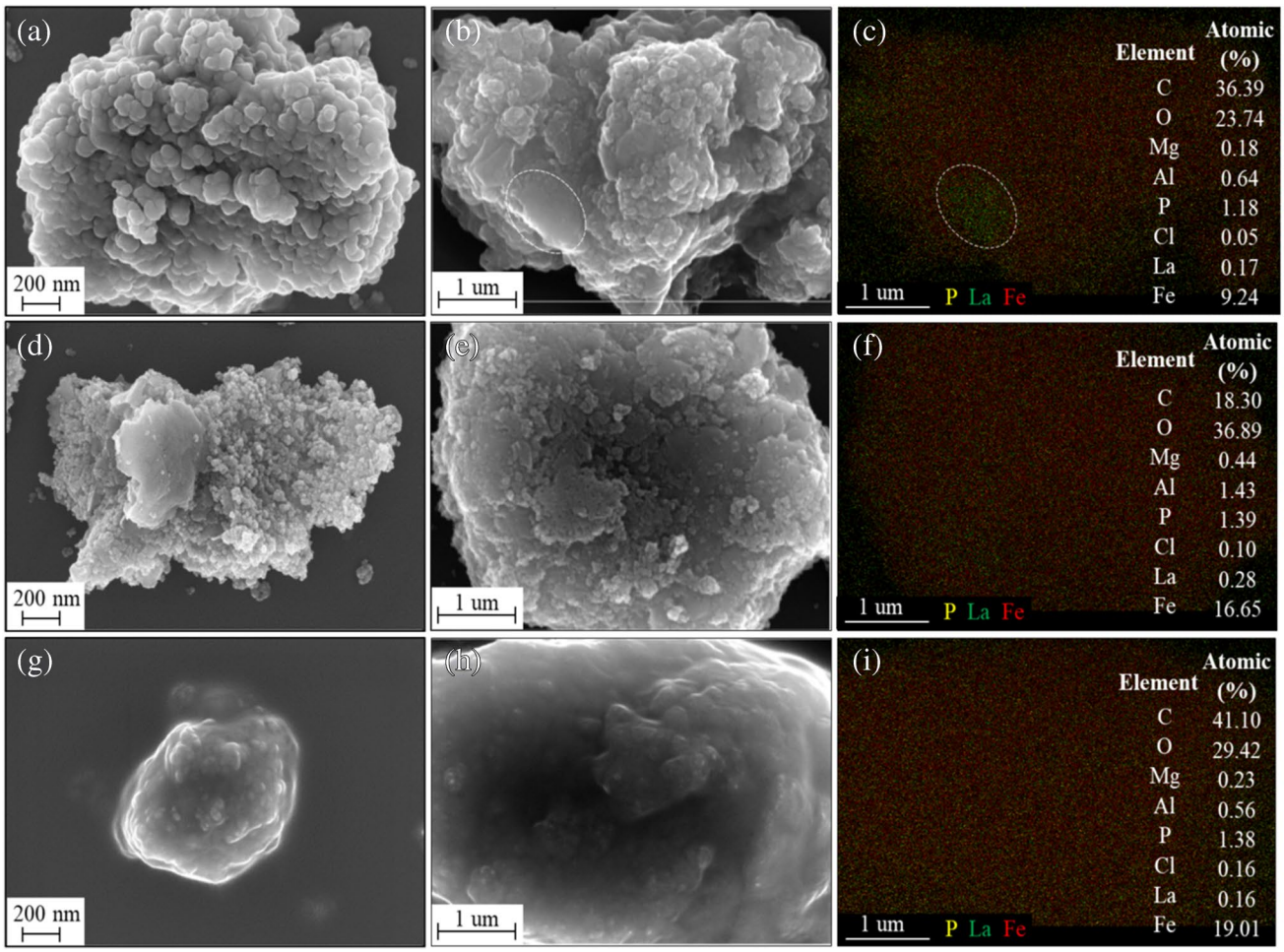

Fig. 9 SEM images and element mapping (yellow P, green La, and red Fe) of (a–c) $M_{26.5}O_{1.7}P_1$, (d–f) $M_{14.9}O_{1.5}P_1$, and (g–i) $M_{6.4}O_{1.4}P_1$ after phosphate adsorption

ammonium (Zhai et al. 2020), which would affect the adsorption performance of phosphate. As shown in Fig. 9 (b) and (c), there is an unoccupied section showing the synchronized distribution of La and P, suggesting that $LaPO_4$ precipitation should be involved for phosphate removal.

Electrostatic interaction with $-R_4N^+$, ligand exchange with hydroxyl groups of Fe_3O_4, and formation of $LaPO_4$ precipitate were proposed to account for the removal of phosphate. The contents of La, Fe_3O_4, and organosilane are decisive factors affecting the adsorption performance of the composites. As aforementioned, electrostatic interactions with $-R_4N^+$ was not the main contributor for phosphate uptake. Thus, only ligand exchange and precipitation are illustrated based on the possible structures of Fe_3O_4@Phoslock® composites (Fig. 10). During the synthesis of composites, (a) the individual organosilane molecule anchored on the surface of Phoslock® and Fe_3O_4 through silylanization reactions, stabilizing the Fe_3O_4 nanoparticles on Phoslock®. In addition, (b) some organosilane cations exchange with La^{3+}, reducing the concentration of La^{3+} and expanding the interlayer space (Fig. 1). However, for those intercalated organosilane molecules, Fe_3O_4 are too large to penetrate to the interlayer space and react with the silane groups. Similar as the case of (a), (c) Fe_3O_4 nanoparticle was firstly grafted by organosilicon molecules and then stabilized by the organosilicon-anchored Phoslock® layers through hydrophobic interactions. At last, slightly different from the case of (b), (d) a fraction of organosilane cations electrostatically anchored on the external surface of Phoslock®, leaving the silane groups available for Fe_3O_4 to achieve further silylanization reactions. No matter the graft of organosilane via electrostatic interaction or silylanization, Fe_3O_4 nanoparticles and Phoslock® became hydrophobic due to the long hydrocarbon chain of organosilane and aggregated together via hydrophobic interactions. Although the content of La^{3+} in $M_{26.5}O_{1.7}P_1$ was the lowest, more Fe_3O_4 made up for the reduced uptake of phosphate. In contrast, $M_{6.4}O_{1.4}P_1$ had the highest La^{3+} concentration but the lowest phosphate uptake, likely because the organosilane film covered the adsorption sites. In general, the adsorption characteristics of three composites were slightly different.

Application test

To further investigate the adsorption performance of phosphate by Fe_3O_4@Phoslock® composites from the real sewage, the landfill leachate treated by Anammox with inorganic P concentration of 3.5 mg/L was applied. $M_{26.5}O_{1.7}P_1$ showed more favorable adsorption performance with respect to the other two. As shown in Fig. 11, the phosphate uptake by three composites increase with the solid–liquid ratio, where the removal rate approximately 75% with the

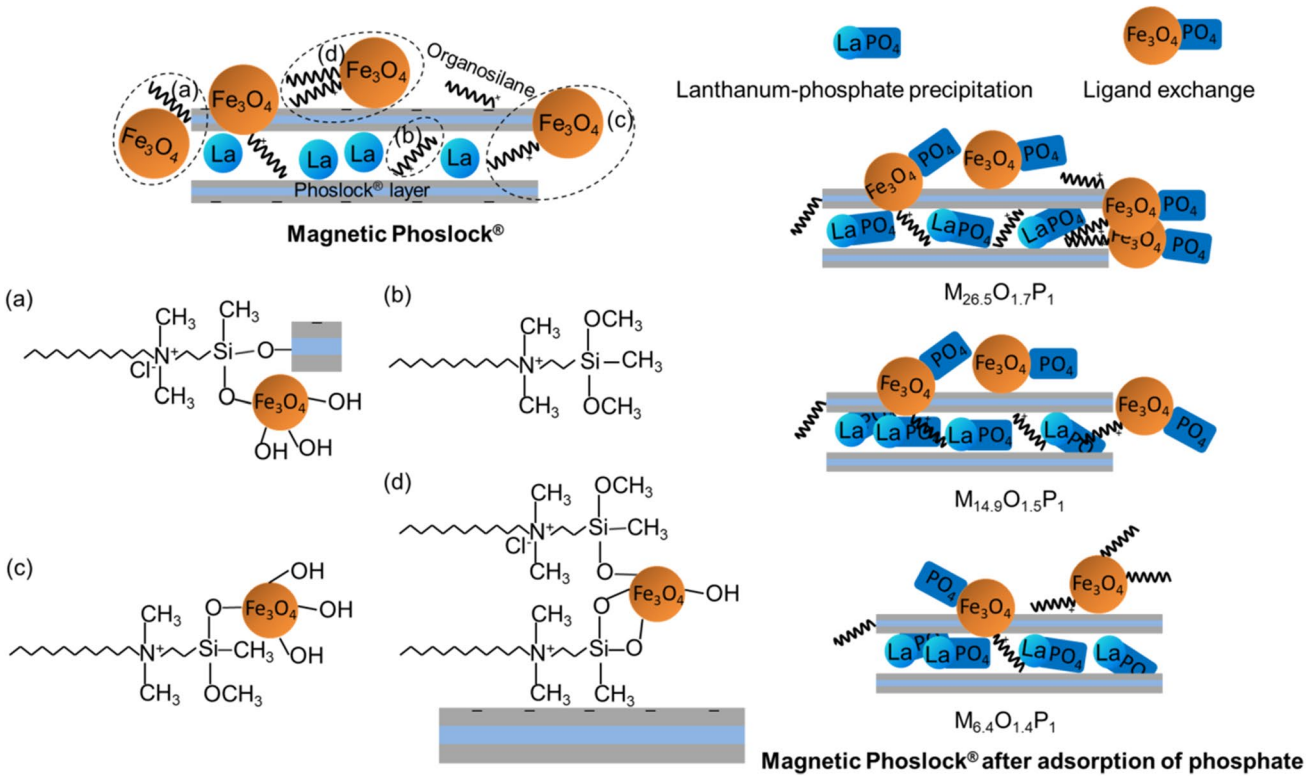

Fig. 10 Schematic illustration of composites structures before and after phosphate adsorption

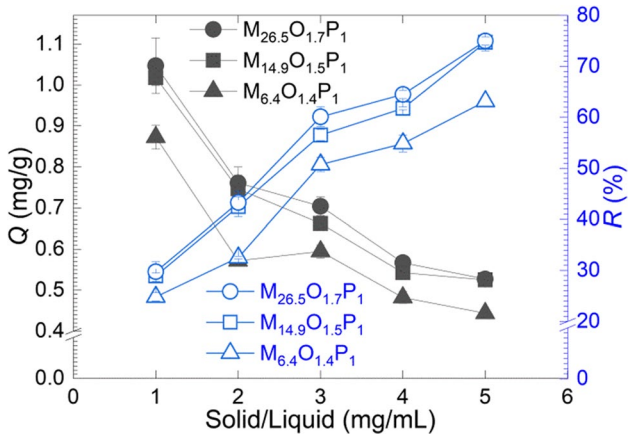

Fig. 11 Effect of adsorbent dosage on the removal of phosphate from landfill leachate treated by Anammox treatment ($V = 10$ mL, $T = 25$ °C, $t = 12$ h, without pH control)

solid–liquid ratio of 5.0 mg/mL was obtained. The sewage pH was around 9.1, which was an important factor affecting the adsorption performance. In addition, due to the complex composition of landfill leachate, the amount of adsorbed phosphate of the composites is reduced.

Conclusions

Three Fe_3O_4@Phoslock® composites (i.e., $M_{26.5}O_{1.7}P_1$, $M_{14.9}O_{1.5}P_1$, and $M_{6.4}O_{1.4}P_1$) with the different contents of Fe_3O_4, organosilane, and Phoslock® were synthesized and applied to study the performance on phosphate adsorption. The better fitting of using pseudo-second order model for the adsorption kinetics suggested the chemical adsorption process, including ligand exchange and precipitation. Due to the heterogeneous adsorption sites, the isothermal data were well fitted by the Freundlich model. All composites showed favorable selectivity and stability against the variation of coexisting ions and solution pH. $M_{26.5}O_{1.7}P_1$ could be easily separated from water for repeated use and had high adsorption capacity for phosphate (~ 20.6 mg/g). In addition, $M_{26.5}O_{1.7}P_1$ could remove 75% of phosphate from landfill leachate treated by Anammox process at dosages of 5 g/L. The adsorbed phosphate could be efficiently desorbed with NaOH solution for at least 5 times.

Author contribution You Mu: investigation, methodology, formal analysis, validation, writing — original draft. Wuhui Luo: conceptualization, resources, supervision, writing — review and editing Zanpeng Cui: investigation. Meng Zhang: resources. Philip Antwi: validation. Dachao Zhang: resources. Sili Ren: supervision, resources.

Funding The study was financially supported by the Program of Qingjiang Excellent Young Talents, Jiangxi University of Science and Technology (JXUSTQJYX2020006), the China Postdoctoral Science Foundation (2018M640604), the Key Research and Development Plan of Jiangxi Province (20203BBG72W007), the Innovative Talent Project of "Thousand Talents Plan" in Jiangxi Province (Jxsq2018101018), and the Key Projects of Natural Science Foundation of Jiangxi Province (20202ACBL203009).

Data Availability All relevant data generated or analyzed during this study were included in this published article.

Declarations

Ethics approval and consent to participate This manuscript does not contain any studies with human participants or animals performed by any of the authors.

Consent for publication Not applicable.

Competing interests The authors declare no competing interests.

References

Aguilar MI, Sáez J, Lloréns M, Soler A, Ortuño JF (2002) Nutrient removal and sludge production in the coagulation–flocculation process. Water Res 36:2910–2919. https://doi.org/10.1016/S0043-1354(01)00508-5

GJ Behets KV Mubiana L Lamberts K Finsterle N Traill R Blust PC D'Haese 2020 Use of lanthanum for water treatment a matter of concern? Chemosphere 239. https://doi.org/10.1016/j.chemosphere.2019.124780

JT Bunce E Ndam ID OfiteruA Moore DW Graham 2018 A review of phosphorus removal technologies and their applicability to small-scale domestic wastewater treatment systems Front Environ Sci 6. https://doi.org/10.3389/fenvs.2018.00008

Chen J, Gao L, Jiang Q, Hou Q, Hong Y, Shen W, Wang Y, Zhu J (2020a) Fabricating efficient porous sorbents to capture organophosphorus pesticide in solution. Microporous Mesoporous Mater 294:109911. https://doi.org/10.1016/j.micromeso.2019.109911

Chen H, Lu C, Yang H (2020b) Lanthanum compounds-modified rectorite composites for highly efficient phosphate removal from wastewater. Appl Clay Sci 199:105875. https://doi.org/10.1016/j.clay.2020.105875

Chen T, Yuan Y, Zhao Y, Rao F, Song S (2019) Preparation of montmorillonite nanosheets through freezing/thawing and ultrasonic exfoliation. Langmuir 35:2368–2374. https://doi.org/10.1021/acs.langmuir.8b04171

Conley DJ, Paerl HW, Howarth RW, Boesch DF, Seitzinger SP, Havens KE, Lancelot C, Likens GE (2009) Controlling eutrophication: nitrogen and phosphorus. Science 323:1014–1015. https://doi.org/10.1126/science.1167755

Cordell D, Drangert J, White S (2009) The story of phosphorus: global food security and food for thought. Glob Environ Chang 19:292–305. https://doi.org/10.1016/j.gloenvcha.2008.10.009

Daou TJ, Begin-Colin S, Grenèche JM, Thomas F, Derory A, Bernhardt P, Legaré P, Pourroy G (2007) Phosphate adsorption properties of magnetite-based nanoparticles. Chem Mater 19:4494–4505. https://doi.org/10.1021/cm071046v

De Gisi S, Lofrano G, Grassi M, Notarnicol M (2016) Characteristics and adsorption capacities of low-cost sorbents for wastewater treatment: a review. Sustain Mater Technol 9:10–40. https://doi.org/10.1016/j.susmat.2016.06.002

Desmidt E, Ghyselbrecht K, Zhang Y, Pinoy L, Van der Bruggen B, Verstraete W, Rabaey K, Meesschaert B (2015) Global phosphorus scarcity and full-scale P-recovery techniques: a review. Crit Rev Environ Sci Technol 45:336–384. https://doi.org/10.1080/10643389.2013.866531

Ding S, Sun Q, Chen X, Liu Q, Wang D, Lin J, Zhang C, Tsang DCW (2018) Synergistic adsorption of phosphorus by iron in lanthanum modified bentonite (Phoslock®): new insight into sediment phosphorus immobilization. Water Res 134:32–43. https://doi.org/10.1016/j.watres.2018.01.055

Długosz O, Banach M (2018) Kinetic, isotherm and thermodynamic investigations of the adsorption of Ag^{+} and Cu^{2+} on vermiculite. J Mol Liq 258:295–309. https://doi.org/10.1016/j.molliq.2018.03.041

Donnert D, Salecker M (1999) Elimination of phosphorus from municipal and industrial waste water. Water Sci Technol 40:195–202. https://doi.org/10.1016/S0273-1223(99)00501-6

Ghosal PS, Gupta AK (2017) Determination of thermodynamic parameters from Langmuir isotherm constant-revisited. J Mol Liq 225:137–146. https://doi.org/10.1016/j.molliq.2016.11.058

AAAM Guerra AFC Campos RM Lima de C Kern FGD Silva G Gomide J Depeyrot AKB Amorim 2020 Efficient uptake of phosphorus from water by core@shellbimagnetic nanoadsorbents J Environ Chem Eng 8. https://doi.org/10.1016/j.jece.2020.103888

Haghseresht F, Wang S, Do DD (2009) A novel lanthanum-modified bentonite, Phoslock, for phosphate removal from wastewaters. Appl Clay Sci 46:369–375. https://doi.org/10.1016/j.clay.2009.09.009

Hokkanen S, Bhatnagar A, Srivastava V, Suorsa V, Sillanpää M (2018) Removal of Cd2+, Ni2+ and PO43− from aqueous solution by hydroxyapatite-bentonite clay-nanocellulose composite. Int J Biol Macromol 118:903–912. https://doi.org/10.1016/j.ijbiomac.2018.06.095

Hu X, Xu J, Wu C, Deng J, Liao W, Ling Y, Yang Y, Zhao Y, Zhao Y, Hu X, Wang H, Liu Y (2017) Ethylenediamine grafted to graphene oxide@Fe_3O_4 for chromium(VI) decontamination: performance, modelling, and fractional factorial design. PLoS ONE 12:e187166. https://doi.org/10.1371/journal.pone.0187166

Kuroki V, Bosco GE, Fadini PS, Mozeto AA, Cestari AR, Carvalho WA (2014) Use of a La(III)-modified bentonite for effective phosphate removal from aqueous media. J Hazard Mater 274:124–131. https://doi.org/10.1016/j.jhazmat.2014.03.023

Kurzbaum E, Shalom OB (2016) The potential of phosphate removal from dairy wastewater and municipal wastewater effluents using a lanthanum-modified bentonite. Appl Clay Sci 123:182–186. https://doi.org/10.1016/j.clay.2016.01.038

Kuzawa K, Jung Y, Kiso Y, Yamada T, Nagai M, Lee T (2006) Phosphate removal and recovery with a synthetic hydrotalcite as an adsorbent. Chemosphere 62:45–52. https://doi.org/10.1016/j.chemosphere.2005.04.015

Lai L, Xie Q, Chi L, Gu W, Wu D (2016) Adsorption of phosphate from water by easily separable Fe_3O_4@SiO_2 core/shell magnetic nanoparticles functionalized with hydrous lanthanum oxide. J Colloid Interface Sci 465:76–82. https://doi.org/10.1016/j.jcis.2015.11.043

F Li J Jin H Ji M Yang 2019 Removal and recovery of phosphate and fluoride from water with reusable mesoporous Fe3O4@mSiO2@mLDH composites as sorbents. J Hazard Mater 388. https://doi.org/10.1016/j.jhazmat.2019.121734

Li H, Ru J, Yin W, Liu X, Wang J, Zhang W (2009) Removal of phosphate from polluted water by lanthanum doped vesuvianite. J Hazard Mater 168:326–330. https://doi.org/10.1016/j.jhazmat.2009.02.025

Y Li H Yen Q Lei W Qiu J Luo S Lindsey L Qin L Zhai H Wang S Wu W Li W Hu H Li H Liu 2020 Impact of human activities on phosphorus flows on an early eutrophic plateau: a case study in Southwest China. Sci Total Environ 714. https://doi.org/10.1016/j.scitotenv.2020.136851

D Liu C Dong J Zhong S Ren Y Chen T Qiu 2020 Facile preparation of chitosan modified magnetic kaolin by one-pot coprecipitation method for efficient removal of methyl orange CarbohydPolym 245. https://doi.org/10.1016/j.carbpol.2020.116572

Liu T, Chen X, Wang X, Zheng S, Yang L (2018) Highly effective wastewater phosphorus removal by phosphorus accumulating organism combined with magnetic sorbent MFC@$La(OH)_3$. Chem Eng J 335:443–449. https://doi.org/10.1016/j.cej.2017.10.117

W Luo Q Huang X Zhang P Antwi Y Mu M Zhang J Xing H Chen S Ren 2020 Lanthanum/Gemini surfactant-modified montmorillonite for simultaneous removal of phosphate and nitrate from aqueous solution. J Water Proc Eng 33. https://doi.org/10.1016/j.jwpe.2019.101036

Mebes B , Ludi C (1989) Production of silyl quaternary ammonium compounds.

Moharami S, Jalali M (2014) Effect of TiO_2, Al_2O_3, and Fe_3O_4 nanoparticles on phosphorus removal from aqueous solution. Environ Prog Sustain Energy 33:1209–1219. https://doi.org/10.1002/ep.11917

Morse GK, Brett SW, Guy JA, Lester JN (1998) Review: Phosphorus removal and recovery technologies. Sci Total Environ 212:69–81. https://doi.org/10.1016/S0048-9697(97)00332-X

Nodeh HR, Sereshti H, Afsharian EZ, Nouri N (2017) Enhanced removal of phosphate and nitrate ions from aqueous media using nanosized lanthanum hydrous doped on magnetic graphene nanocomposite. J Environ Manage 197:265–274. https://doi.org/10.1016/j.jenvman.2017.04.004

Othman A, Dumitrescu E, Andreescu D, Andreescu S (2018) Nanoporous sorbents for the removal and recovery of phosphorus from eutrophic waters: sustainability challenges and solutions. ACS Sustain Chem Eng 6:12542–12561. https://doi.org/10.1021/acssuschemeng.8b01809

Peng J, Liu Q, Xu Z, Masliyah J (2012) Synthesis of interfacially active and magnetically responsive nanoparticles for multiphase separation applications. Adv Func Mater 22:1732–1740. https://doi.org/10.1002/adfm.201102156

Pjurova B, Raclavska H, Skrobankova H (2013) Ecotoxicity of nanomaterials on the basis of clay minerals. Adv Mater Res 853:282–287. https://doi.org/10.4028/www.scientific.net/AMR.853.282

Rittmann BE, Mayer B, Westerhoff P, Edwards M (2011) Capturing the lost phosphorus. Chemosphere 84:846–853. https://doi.org/10.1016/j.chemosphere.2011.02.001

Robb M, Greenop B, Goss Z, Douglas G, Adeney J (2003) Application of phoslock tm, an innovative phosphorus binding clay, to two western australian waterways: preliminary findings. Hydrobiologia 494:237–243. https://doi.org/10.1023/A:1025478618611

Ross G, Haghseresht F, Cloete TE (2008) The effect of pH and anoxia on the performance of Phoslock®, a phosphorus binding clay. Harmful Algae 7:545–550. https://doi.org/10.1016/j.hal.2007.12.007

Sengupta S, Nawaz T, Beaudry J (2015) Nitrogen and phosphorus pecovery from wastewater. Curr Pollut Rep 1:155–166. https://doi.org/10.1007/s40726-015-0013-1

Spears BM, Lürling M, Yasseri S, Castro-Castellon AT, Gibbs M, Meis S, McDonald C, McIntosh J, Sleep D, Van Oosterhout F (2013) Lake responses following lanthanum-modified bentonite clay (Phoslock®) application: an analysis of water column lanthanum data from 16 case study lakes. Water Res 47:5930–5942. https://doi.org/10.1016/j.watres.2013.07.016

Tu Y, You C, Chang C, Chen M (2015) Application of magnetic nanoparticles for phosphorus removal/recovery in aqueous solution. J Taiwan Inst Chem Eng 46:148–154. https://doi.org/10.1016/j.jtice.2014.09.016

Van Vuuren DP, Bouwman AF, Beusen AHW (2010) Phosphorus demand for the 1970–2100 period: a scenario analysis of resource depletion. Glob Environ Chang 20:428–439. https://doi.org/10.1016/j.gloenvcha.2010.04.004

Wen T, Wu X, Tan X, Wang X, Xu A (2013) One-pot synthesis of water-swellable Mg–Al layered double hydroxides and graphene oxide nanocomposites for efficient removal of As(V) from aqueous solutions. ACS Appl Mater Interfaces 5:3304–3311. https://doi.org/10.1021/am4003556

Wendling LA, Blomberg P, Sarlin T, Priha O, Arnold M (2013) Phosphorus sorption and recovery using mineral-based materials: sorption mechanisms and potential phytoavailability. Appl Geochem 37:157–169. https://doi.org/10.1016/j.apgeochem.2013.07.016

CY Wong IS Tan HCY Foo DKH Tang YH Tan YF Yeong MK Lam 2020 Monolayer grafting of APTES modified graphene oxide on silica coated magnetite: synthesis, characterization and application in heavy oil removal IOP Confer Ser Mater SciEng 943. https://doi.org/10.1088/1757-899X/943/1/012023

Xie F, Da C, Zhang F, Zhang J, Han X, Ge Y, Li G (2013) Phosphorus removal from eutrophic waters with a novel lanthanum-modified diatomite. Asian J Chem 25:5759–5761. https://doi.org/10.14233/ajchem.2013.oh84

Yamada-Ferraz TM, Sueitt APE, Oliveira AF, Botta CMR, Fadini PS, Nascimento MRL, Faria BM, Mozeto AA (2015) Assessment of Phoslock® application in a tropical eutrophic reservoir: An integrated evaluation from laboratory to field experiments. Environ Technol Innov 4:194–205. https://doi.org/10.1016/j.eti.2015.07.002

Yang J, Zeng Q, Peng L, Lei M, Song H, Tie B, Gu J (2013) La-EDTA coated Fe_3O_4 nanomaterial: Preparation and application in removal of phosphate from water. J Environ Sci 25:413–418. https://doi.org/10.1016/S1001-0742(12)60014-X

Yoon SY, Lee CG, Park JA, Kim JH, Kim SB, Lee SH, Choi JW (2014) Kinetic, equilibrium and thermodynamic studies for phosphate adsorption to magnetic iron oxide nanoparticles. Chem Eng J 236:341–347. https://doi.org/10.1016/j.cej.2013.09.053

Zhai M, Wu M, Wang C, Li X (2020) A novel silica-supported polyether polysiloxane quaternary ammonium demulsifier for highly efficient fine-sized oil droplet removal of oil-in-water emulsions. RSC Adv 10:18918–18926. https://doi.org/10.1039/d0ra01679a

Publisher's Note Springer Nature remains neutral with regard to jurisdictional claims in published maps and institutional affiliations.